Journal of The Electrochemical Society, **152** (10) F162-F170 (2005)
0013-4651/2005/152(10)/F162/9/$7.00 © The Electrochemical Society, Inc.

Plasma Treatment and Surface Analysis of Polyimide Films for Electroless Copper Buildup Process

Dhananjay Bhusari,[a,z] Harley Hayden,[a,*] Ravindra Tanikella,[b] Sue Ann Bidstrup Allen,[a,] and Paul A. Kohl[a,***]**

[a]*School of Chemical and Biomolecular Engineering, Georgia Institute of Technology, Atlanta, Georgia 30332-0100, USA*
[b]*Intel Corporation, Assembly Technology Development, Chandler, Arizona 85226, USA*

We report here a detailed characterization of the surface chemical states and morphology of polyimide (PI) films following modifications by plasma treatment and electroless copper deposition. NH_3 and Ar plasma treatments have been successfully used to achieve morphological and chemical modification of the PI surface so that electroless copper plating can occur. The adhesion strength of the electroless copper to the PI surface was measured and correlated with the plasma-induced chemical and physical modifications of the PI surface. The NH_3 plasma causes primarily chemical changes to the PI surface through creation of nitrogen moieties (i.e., –N═C<) on the surface. The Ar plasma treatment brings about mainly physical changes to the surface (i.e., surface roughening). The combined-plasma treatment (Ar plasma followed by NH_3 plasma) combines the desirable chemical and physical effects of each treatment, yielding a PI surface with higher roughness for physical anchoring of the copper and surface bonding sites (nitrogen and oxygen sites). During the electroless copper surface activation step with tin chloride and palladium chloride, tin bonds mainly with the oxygen on the surface, whereas palladium reacts with tin chloride as well as with the surface nitrogen. A direct relationship has been observed between surface palladium concentration and the abundance of the –N═C< sites on the surface. This suggests that the nitrogen radicals created during the NH_3 plasma are incorporated into the surface and serve as bonding sites for the palladium. In the subsequent electroless Cu deposition, there was a direct correlation between the palladium surface concentration and Cu coverage. The adhesion strength of the electroless copper to the PI correlated well to the surface modifications and plasma treatment conditions. For the first time, a specific bonding configuration on the PI surface is shown to promote adsorption of palladium, which in turn promotes covalent bonding with Cu. The relative importance of surface roughness and chemical bonding on the adhesion strength is discussed.
 [DOI: 10.1149/1.2006587]

Manuscript submitted February 4, 2005; revised manuscript received April 15, 2005. Available electronically August 25, 2005.

Electroless metallization of advanced low-*k* polymers is of great interest for future high-density packaging substrates. Polyimides (PI) are an important class of polymers with desirable properties for these packaging and interconnect applications. However, PIs are difficult to activate for subsequent electroless metallization via conventional chemical "swell and etch" treatments.[1] These treatments are widely used for activating epoxy substrates and provide excellent adhesion strength between the electroless copper and the epoxy. Adhesion peel strengths on the order of 460 N/m have been reported for Cu on epoxy substrates.[2] Since the conventional swell and etch treatment has been found to be ineffective to activate the PI surface for electroless Cu deposition, several alternative surface treatments have been attempted in order to activate the PI surfaces. In work performed by Okamura et al.,[3] a KOH treatment has been used to cleave the imide ring of the PI creating carboxyl and amide groups on the PI surface, which presumably enhances the adhesion with electroless copper. However, this treatment not only affects the surface of the polymer but also cleaves the imide rings deep in the material if the treatment time is not closely controlled. This study indicates that combining the KOH treatment with a standard swell and etch process improves the adhesion by a factor of 5 to a value of ~150 N/m. Modification of the PI by graft copolymerization with amines has been attempted in order to add the adhesion promoting groups to the PI backbone.[4-7] This approach has improved the adhesion strength between copper and PI to 40–60 N/m. Adhesive layers of other metals such as chromium, zinc, tin, and indium have been used at the PI—electroless metal interface, and the strength of adhesion improved to several hundred N/m.[8-10]

The use of plasma treatment to produce chemical and physical surface modifications of polymers has been widely reported. PIs have been subjected to Ar, O, N, and NH_3 plasma treatments in order to make the polymer surface more reactive toward electroless copper deposition and improve adhesion.[11-16] Ion-beam treatment of PIs with oxygen, nitrogen, and argon ions has been reported to increase the surface concentration of the respective species at low ion energies, while high ion energies result in differential sputtering, leaving the surface carbon rich.[13] The argon-ion reactive ion etching (RIE) treatment has been shown to decrease the surface nitrogen and oxygen concentration and results in rearrangement of the surface nitrogen bonding to form >C═N– and pyridinelike species on the PI surface.[15] Oxygen RIE treatment has been shown to increase the surface oxygen concentration by 70–180%, while nitrogen and carbon concentrations decrease by 10–30%. The oxygen plasma treatment is also reported to increase the oxygen surface concentration and increase the carbonyl bonding on the surface.[16] Further, interactions of the modified and unmodified PI surfaces with various metals such as chromium, aluminum, germanium, and copper have also been studied for electroless copper deposition.[17-20] The increase in surface nitrogen concentration brought about by N_2 or NH_3 plasma treatment has been found to be beneficial, resulting in improved adsorption of the catalysts Sn and Pd.[21] Nevertheless, a detailed study of the modification in surface chemical composition and morphology of PI surface with various plasma treatments has not been reported so far. Further, a detailed understanding of the interactions between surface chemical states of PI and metals such as tin, palladium, and copper is also necessary to improve the adhesion strength between PI and copper. In this study a detailed analysis of the PI surface with different plasma treatments, viz., NH_3 plasma and Ar RIE, through each step of the electroless copper deposition process has been carried out. For the first time, correlations between certain specific bonding moieties on the PI surface and palladium adsorption have been made. The peel strength of copper has been improved to 60 N/m without significantly damaging the PI surface.

Experimental

PI 2555 from HD Microsystems (BTDA-ODA-MPD structure-3,3′,4,4′-benzophenone tetracarboxylic dianhydride 4,4-oxydianiline *m*-phenylene diamine) was spin coated onto silicon substrates at a spin speed of 1000 rpm to yield 8-μm-thick films. Adhesion promoter (VM-652) was spin coated onto the silicon wafers prior to coating the PI. The PI film was soft baked at 100°C in air,

* Electrochemical Society Student Member.
** Electrochemical Society Member.
*** Electrochemical Society Fellow.
z E-mail: dbhusari@chbe.gatech.edu

followed by curing at 350°C for 1 h in N_2 atmosphere. The plasma treatments were carried out in a Plasma-Therm chamber. The typical NH_3 plasma treatment parameters were 20 sccm NH_3 flow rate, 200 mTorr chamber pressure, 150°C substrate temperature, 30–80 W rf power, and 0.5 to 5 min treatment times. The Ar RIE parameters were 200 sccm Ar flow rate, 250 mTorr chamber pressure, 25°C substrate temperature, 50–400 W rf power, and 5 min treatment time. Following the plasma treatment, the samples were activated with the Sn/Pd catalyst (Shipley Cataposit 44) at 46°C for 20 min followed by rinsing with deionized water. Finally, the samples were electrolessly copper plated with 1 μm copper (Shipley Circuposit 3350) at 46°C. The copper thickness was increased for the peel tests by electroplating an additional 40 μm of copper.

The adhesion strength of the copper to the PI was measured with a 90° peel test using an Instron (model 5842) instrument following the ASTM B 533-85 standard. In this test, a 5-mm-wide strip of copper was pulled at the rate of 25 mm/min, and the average force was calculated to yield the peel strength in N/m. The surface analyses were carried out using a Perkin Elmer XPS system (model PHI 1600) and Veeco AFM (model Nanoscope IIIa) in the tapping mode. The AFM tip diameter was 40 nm. The surface chemical composition of the films was determined from the X-ray photoemission spectroscopy (XPS) spectra based on the integrated area under the photoelectron peak of each element and their respective sensitivity factors (photoelectron emission cross section). All elements that displayed peaks in the XPS survey scan were included in the chemical composition calculations. The effect of XPS sampling depth and its possible variation with surface metal coverage was not taken into consideration.

Results and Discussion

PI films were subjected to one of three plasma treatments: NH_3 plasma, Ar RIE, and a combination of Ar RIE followed by NH_3 plasma. These treatments were selected to study the effect of chemical and physical changes of the PI surface on adhesion and other properties. The NH_3 plasma treatment was expected to primarily result in chemical modification of the PI surface, because the plasma contained chemically reactive nitrogen radicals, and the treatment was carried out under low plasma power (e.g., 30 to 80 W). At these low powers, ion bombardment was minimal. The Ar RIE treatment resulted in mainly physical roughening of the surface with little chemical modification, because the Ar ions generated in this plasma are known to cause mainly sputter etching of the surface. Becasue the substrates are kept on a powered electrode in this process, the energy of ion bombardment on the substrates is much higher than the usual rf plasmas, where substrates are kept on a grounded electrode. Any chemical modification in this process is a result of differential sputtering and ion-bombardment induced reordering. Treating the PI surface with both plasma treatments that induce physical and chemical changes was investigated. The process parameters in the combined plasma treatment (i.e., power, pressure, and time) were varied in order to achieve optimum results.

The XPS survey scans for four samples: (*i*) untreated PI; (*ii*) 80 W NH_3 plasma; (*iii*) 150 W Ar plasma; and (*iv*) 150 W Ar plasma followed by 30 W NH_3 plasma, are shown in Fig. 1. These scans show the presence of C, O, and N peaks in all spectra, as expected. Traces of a silicon impurity from residuals in the chamber were also observed. The chemical shift will be discussed later in this paper.

The AFM scans of the corresponding surfaces are shown in Fig. 2. The untreated PI surface is very smooth, with a root-mean-square (rms) roughness of only 4.2 Å (measured on a 1-μm-square area). The roughness increased to 29.3 Å for the 80 W NH_3 plasma treatment. The roughness after the 150 W plasma treatment was 175.5 Å and increased to 183.2 Å for the combined plasma treatment (150 W Ar plasma and 30 W NH_3 plasma treatment).

The atomic concentration of C, O, and N on the PI surface, as calculated from the XPS spectra, and the rms surface roughness are

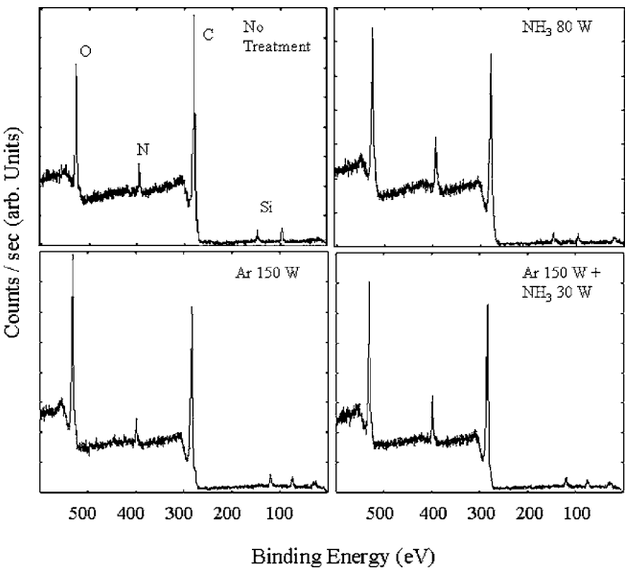

Figure 1. XPS spectra of PI samples with different plasma treatments.

plotted in Fig. 3. The NH_3 plasma treatment results in a carbon depleted surface. The carbon signal decreased from 80 atom % in the untreated sample to 61 atom % at 30 W power, and 66 atom % at 80 W. The oxygen concentration increased from 15% in the untreated sample to 25% for the 30 W treatment and 20.5% at 80 W. These results, along with the increase in surface roughness, suggest that C is etched by the NH_3 plasma, especially at lower power. As the plasma power increased, the oxygen etching increased relative to that of carbon, resulting in a gradual increase in the relative fraction of carbon to oxygen on the surface. The nitrogen content increased from 4.1 atom % for the untreated sample to 10.5 atom % for the 80 W treatment. The nitrogen radicals generated in the plasma react with the surface and form covalent nitrogen bonds at energetically favorable sites. The higher the plasma power, the higher the density of nitrogen radicals, leading to an increased concentration of nitrogen. Thus, the NH_3 plasma produces a PI surface with a higher nitrogen content and marginally higher surface roughness compared to the untreated surface.

The carbon concentration on the surface after the Ar plasma treatment also decreased while the amount of oxygen and nitrogen increased with plasma power, indicating that carbon is sputtered at a higher rate than oxygen and nitrogen. The decrease in carbon and increase in nitrogen are more gradual than with the NH_3 plasma treatment. The highest concentration of oxygen occurred at 50 W, indicating that the sputtering rate of oxygen increased with power, as seen with the NH_3 plasma treatment. Thus, the Ar plasma treatment produces a PI surface with slightly higher oxygen and nitrogen concentrations and significantly higher roughness.

The sequential Ar and NH_3 plasma treatments resulted in a higher nitrogen content (14%) than the single NH_3 plasma treatment. This can be attributed to additional nitridation of the surface by NH_3 plasma after the Ar plasma treatment. It is also possible that the Ar plasma treatment creates sites on the surface that are more reactive to the nitrogen radicals when subjected to the subsequent NH_3 plasma treatment. The surface roughness increased only slightly compared to the single Ar plasma treatment. Thus, the combined plasma treatment yielded a PI surface rich in nitrogen and oxygen and with high roughness. These results demonstrate that the chemical composition and physical texturing of the PI surface can be controlled independently by using NH_3 and Ar plasma treatments, respectively. It is also possible to achieve a specific combination of surface composition and roughness by altering the conditions for the two treatments.

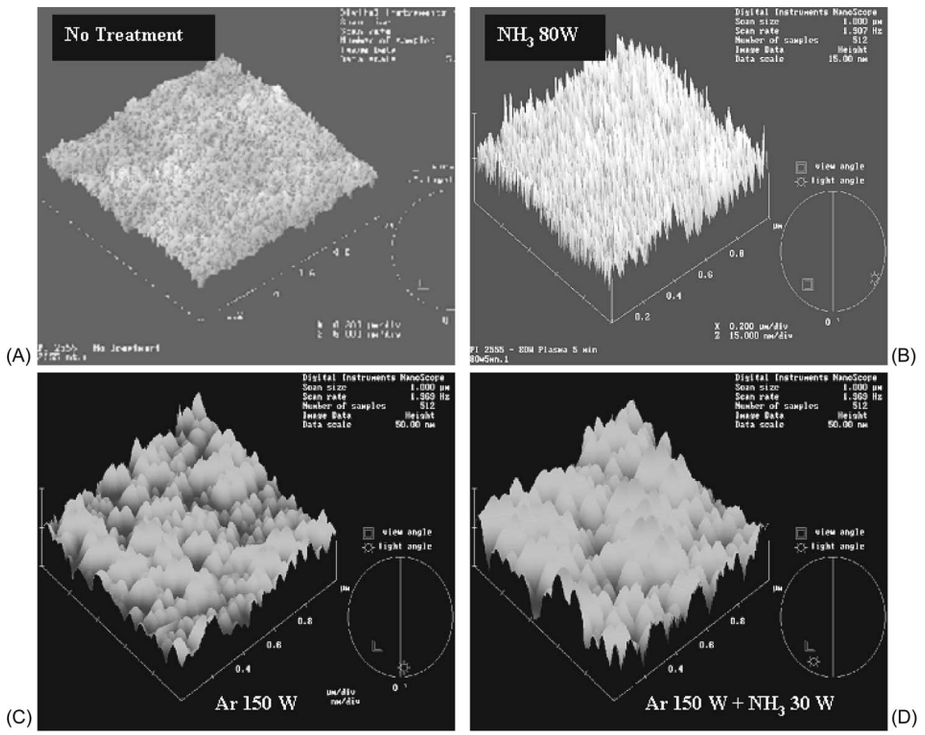

Figure 2. Variations in the surface roughness of PI films with different plasma treatments (A) No treatment: R_{rms} = 4.2 A; (B) NH_3 80 W: R_{rms} = 29.3 A; (C) Ar 150 W: R_{rms} = 175.5 A; and (D) Ar 150 W + NH_3 30 W: R_{rms} = 183.2 A.

The details of the chemical bonding states of the carbon, oxygen, and nitrogen have also been studied by analyzing the core-level XPS spectra of the elements. Figure 4 shows the core level spectra of carbon, oxygen, and nitrogen for the untreated PI sample. The chemical composition of the untreated sample is C: 80.3%, O: 15%, and N: 4.1%. This is within experimental error of the composition of PI, C: 78.1%, O: 15.6%, and N: 6.2%. The C peak is comprised of three component peaks belonging to the three bonding states of carbon in the polymer:[22] C–C at 284.7 eV (peak 1), C–N at 285.5 eV (peak 2), and C═O at 288.3 eV (peak 3). The relative fractions of these components are C–C: 78.9%, C–N: 11.5%, and C═O: 9.6%. The theoretical values of these components in PI are C–C: 71.4%, C–N: 15.6%, and C═O: 13%. The higher fraction of C–C and lower fractions of C–N and C═O in the untreated film compared to the theoretical values are probably due to the lower O and N concentrations in the spin-coated film, as previously noted. The O peak is comprised of two components:[22] O═C at 531.9 eV (peak 1-84.6%) and O–C at 533.2 eV (peak 2-15.4%). Theoretically, all O should be in the O═C state and there should be no O–C.

The nitrogen core-level spectrum also exhibits two components: 398.5 eV (peak 2-19.2%), and 400.2 eV (peak 1-80.8%). In this PI, nitrogen is only found in the N–C configuration (400.2 eV); however, because carbon which can be bonded to nitrogen is found in two forms, the corresponding nitrogen can have two states, viz., the aromatic ring (>C–C <) and the carbonyl group (>C═O). Several publications have reported such a shift in the nitrogen core-level spectrum;[13,15,23] however, the 398.5 eV peak has not been discussed in detail. We believe that the component at 400.2 eV belongs to N–C═O bonding, as commonly reported in the literature, while the peak at 398.5 eV belongs either to N–C–C bonding or is caused due to the incomplete imidization of the polymer. Although the order of electronegativity of C, N, and O supports the assignment of the 398.5 eV peak to N–C–C bonding, it is somewhat difficult to imagine that variation in the C bonding environment from C–C to C═O would cause such a large secondary shift of 1.7 eV in the N 1s binding energy.

Figure 5 shows the carbon, oxygen, and nitrogen core-level spectra after the 80 W NH_3 plasma treatment. A comparison of these spectra with those of the untreated sample (Fig. 4) reveals major changes in the carbon and nitrogen peaks. In the carbon peak, the relative fraction of the C–N component (peak 2 in the carbon spectra) increased from 11.5% in the untreated sample to 19.2% in the plasma-treated sample, indicating that the N implanted by the plasma is bonded to carbon. In addition, two new peaks appear at 286.3 eV (peak 4) and 283.4 eV (peak 5), belonging to C–O and C–Si bonding, respectively. The formation of C–O is probably a derivative of C═O bonds after ion bombardment. The C–Si structures are due to the silicon contamination of the surface from the plasma chamber, as noted earlier. The plasma treatment lowers the C–C content (peak 1 in the carbon spectra) from 78.9% in the untreated sample to 48.9% in the plasma-treated sample. This shows that cleavage of a significant number of C–C bonds occurs in the plasma process. The relative fraction of C═O (peak 3 in the carbon spectra) increases from 9.6% in the untreated sample to 15.4% in the plasma treated sample. This suggests that the carbon in the C═O form is etched at a lower rate than that in the aromatic ring, leaving more C═O groups on the surface, which is consistent with the higher dissociation energy of the C═O bond than the C–C bond. Oxygen, in the form of O–C (peak 2 in the oxygen spectra), increased from 15.4% for the untreated sample to 27.1% for the 80 W NH_3-treated sample. A new peak at 530.5 eV (peak 3 in oxygen spectrum), belonging to O–Si bonding, also appears due to surface contamination. The nitrogen peak shows the greatest change. A new contribution (33.5%) appears at 399.5 eV (peak 3 in the nitrogen spectrum), which has been assigned to linear –N═C< species in the literature.[15] The fraction of these new N═C moieties increases with plasma power from 30 to 80 W. The assignment of 399.5 eV to N═C bonding is somewhat controversial. In fact, chemical shifts in the N 1s photoelectron peak with variations in the N bonding environment are relatively smaller in magnitude than O and C photoelectron peaks. Consequently, variations in the N bonding environment are often difficult to distinguish based solely on the N 1s spectrum. Secondary shifts (bonding environment of the atoms that are bonded to N) often dictate the N 1s binding energy in several polymers.[22] It is also difficult to resolve this new N═C bonding in the C 1s spectrum, because the C 1s peak already consists of five

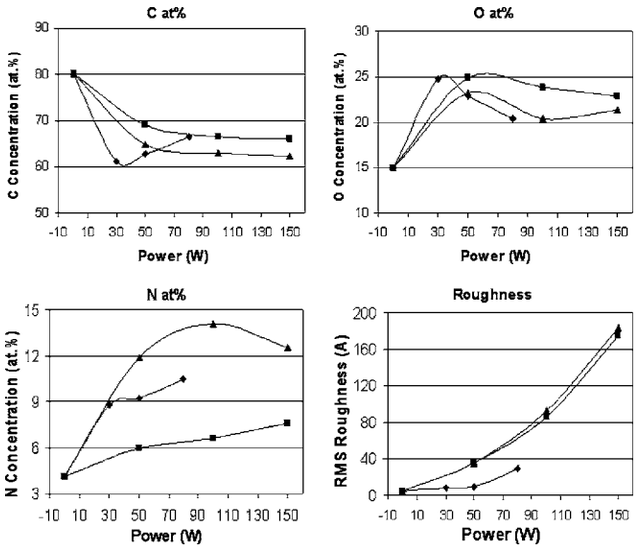

Figure 3. Variations in the surface concentrations of C, O, and N and surface roughness of the PI films with plasma power (◆-NH_3 plasma, ■-Ar plasma, and ▲-Ar + NH_3 plasma).

component peaks and C═N would appear very close in energy to C–N. We assign the 399.5 eV peak to linear >C═N-moieties based on the results of Flitsh et al.,[15] but this assignment may not be unique, since C≡N also appears close in energy at 399.6–399.7 eV in some polymers.[22]

Figure 6 shows the carbon, oxygen, and nitrogen core level spectra for the PI sample treated with 150 W Ar plasma. The Ar plasma treatment was carried out in the RIE mode, where the substrates are held on a powered electrode, so that the energy of the ions bombarding the surface is much higher than the earlier NH_3 plasma treatment. The kinetic energy of the ions induces physical sputter etching, which leads to an increase in surface roughness as compared to the NH_3 plasma treatment. Figure 2 shows the increase in surface roughness. Thus, there can be significant rearrangement of the bonding states on the Ar etched surface. Figure 3 shows that the carbon content decreases continuously with plasma power for the Ar etched sample, while the concentrations of oxygen and nitrogen increase. The carbon peak in Fig. 6 shows a decrease in the concentration of the C–C component (peak 1 in carbon spectra) to 59.0%, while that of the C–N (peak 2) and C═O (peak 3) components increases to 15.4 and 16.4%, respectively. The overall surface composition is C (66.0%), O (22.9%), and N (7.6%), as shown in Fig. 3. The increase in surface concentration of nitrogen in this case is much less than that with the NH_3 plasma treatment. This increase in the nitrogen surface concentration causes an increase in the concentration of the C–N component, as seen in the carbon spectra in Fig. 6. Further, the increase in concentration of the C═O (peak 3) component suggests

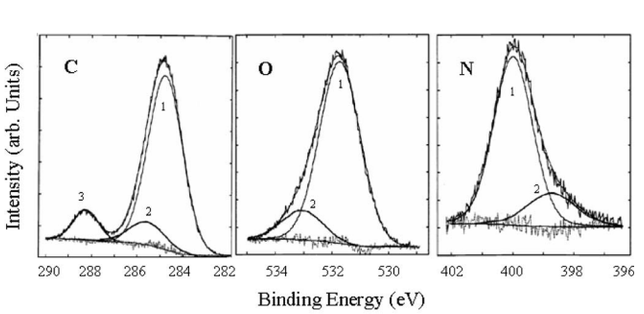

Figure 4. Core-level XPS spectra of C, O, and N in untreated PI films.

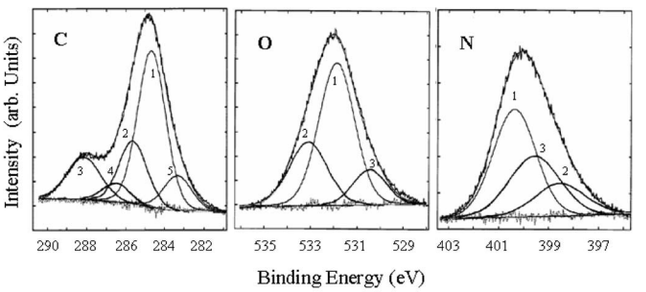

Figure 5. C, O, and N core-level XPS spectra after 80 W NH_3 plasma treatment.

that the C in the carbonyl group is etched at a lower rate than the carbon in the aromatic ring, similar to observations from the NH_3 plasma treatment. The oxygen peak in Fig. 6 does not display any major change compared to the untreated samples (Fig. 4), except for the marginal increase in the concentration of the C–O component (peak 2) from 15.4 to 21.2%. This is consistent with the appearance of the C–O peak in the carbon spectrum. The N peak shows a significant decrease in the fraction of N–C–C bonding (peak 2) due to the etching of carbon from the aromatic ring, and formation of the new peak at 399.5 eV (peak 3). This was also observed in the NH_3 plasma treatment, although to a greater extent than the Ar plasma (33.5% in NH_3 plasma vs 21.3% in Ar plasma). The formation of this new peak at 399.5 eV, belonging to N═C, indicates that there is significant rearrangement of N on the surface as a result of ion bombardment and sputter etching. A similar nitrogen rearrangement with the Ar plasma has been reported by Flitsch et al.[15] Formation of N═C in the NH_3 treatment is a result of chemical reaction between surface moieties and plasma-generated radicals. Thus, the Ar plasma treatment increases the C═O and C═N bonding, in addition to roughening the surface.

Figure 7 shows the carbon, oxygen, and nitrogen spectra after the combined plasma treatments (i.e., 150 W Ar followed by 30 W NH_3). In this sample, the overall surface composition is C (62.4%), O (21.4%), and N (12.5%). The C spectrum contains the signature of both plasma treatments: a C–N fraction (peak 2) as high as 18%, and a C═O fraction (peak 3) at 18.1%. The C–O fraction (peak 4) increased to 9.9%, compared to 0% in the untreated sample, 5.8% in the NH_3 80 W sample, and 6% in the Ar 150 W sample. These results are consistent with the oxygen spectrum, where the concentration of C–O (peak 2-28.2%) is higher than in either of the individual plasma treatments. The nitrogen spectrum displays a very strong C═N component (peak 3) at 399.5 eV (37.4%), which is higher than the NH_3 80 W sample. Again, the nitrogen inserted by the NH_3 plasma is bonded in the form of N═C. Thus, the combination of Ar and NH_3 plasma treatments yields a PI surface that is rich in nitrogen and oxygen with high surface roughness.

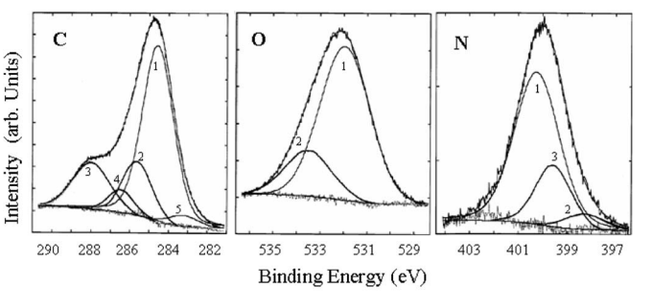

Figure 6. C, O, and N core-level XPS spectra after 150 W Ar plasma treatment.

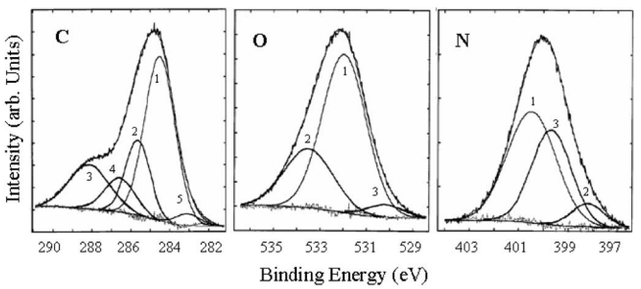

Figure 7. C, O, and N core-level XPS spectra after combined plasma treatment with 150 W Ar followed by 30 W NH_3.

For comparison, the chemical and physical changes of the PI surface after the conventional swell and etch treatment were also studied. The samples were "swelled" in the sweller solution (Shipley Circuposit 3302) at 80°C for 10 min and etched (in Shipley Circuposit 3308) at 80°C for 5 and 30 min. The AFM scans for these samples showed the rms surface roughness increasing from 4.1 Å in the untreated surface to 7.3 Å for 5 min treatment and to 11.1 Å for the 30 min treatment. This increase in roughness is lower than that observed by the Ar plasma treatments (see Fig. 2). This treatment did not cause any significant change in the surface chemical structure either. The composition of the surface after the 5 min treatment was C (75.7%), O (15.6%), and N (4.9%), while after a 30 min treatment it was C (75.2%), O (18.3%), and N (4.3%). Thus, the swell and etch treatment increased the surface oxygen concentration slightly from 15 to 18.3%, decreased the carbon concentration from 80.3 to 75.2%, and had a negligible effect on nitrogen fraction. Thus, the wet treatment was found to be ineffective in chemical as well as morphological modification of the PI surface, in agreement with the literature.[1]

Following the plasma treatments, the samples were subjected to a Sn–Pd activation-sensitization step. It has been reported in the literature[21] that the chemically etched or oxygen plasma-treated PI surface produces Sn atoms primarily bonded to the surface oxygen via the C═O groups to form C–O–Sn linkages. The palladium chloride is reduced by the tin(II) and adheres to the surface. On the nitrogen plasma-treated surfaces, however, palladium has been reported to bond with the surface nitrogen, in addition to the C–O– linkage.[21] The N-plasma-treated PI surfaces are reported to adsorb a higher amount of Pd than either the wet treatments or O-plasma-treated surfaces. Further, the higher Pd coverage on the surface is believed to be beneficial to Cu nucleation and adhesion because Cu deposition is initiated by Pd in the copper electroless process. Cu does not react with the surface C═O groups to form the C–O-metal linkage,[17] and reacts very weakly with N.[23] The amount of Sn and Pd adsorbed on the surface and their oxidation states on the surface were measured for different plasma treatments in order to understand their bonding on the surface. The XPS survey scans after the Sn–Pd activation step are shown in Fig. 8 for three samples with different plasma treatments: NH_3 80 W, Ar 150 W, and Ar 150 W + NH_3 30 W.

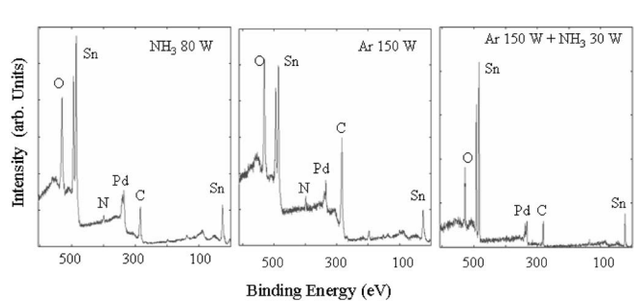

Figure 8. XPS survey scans of NH_3 80 W, Ar 150 W, and Ar 150 W + NH_3 30 W plasma treated PI samples after the Sn–Pd activation step.

Table I. Surface chemical compositions of PI samples (in atom %) subjected to different plasma treatments before and after the Sn–Pd activation.

Surface treatment		C	O	N	Sn	Pd
No Treat		80.3	15	4.1		
30 W NH_3		61.1	24.8	8.8		
	Sn–Pd	44.8	40.9	4.5	7.9	1.7
80 W NH_3		66.4	20.4	12.3		
	Sn–Pd	34.2	41.8	3.3	16.2	4.3
50 W Ar		69.1	24.9	6.5		
	Sn–Pd	55.9	30.1	6	7.3	0.7
150 W Ar		66	22.9	7.6		
	Sn–Pd	58.4	28.6	4.3	7.6	1.2
50Ar + 30NH		64.8	23.2	11.9		
	Sn–Pd	33.7	39.7	4.3	17.6	3.5
150Ar + 30NH		62.4	21.4	12.5		
	Sn–Pd	31.7	40.5	3.2	21.1	4.7

The prominent peaks belonging to Sn and Pd can be seen in Fig. 8 at 486 and 337 eV, respectively. This confirms the adsorption of Sn as well as Pd on the plasma-treated PI surfaces. There are major changes in the surface concentrations of the carbon, oxygen, and nitrogen after the Sn–Pd step for each of the plasma treatments. The surface composition of all plasma-treated samples before and after the Sn–Pd treatment is shown in Table I. Overall, there is significant reduction in the concentration of carbon and nitrogen and an increase in oxygen. The NH_3 80 W and Ar 150 W + NH_3 30 W treatments show a greater decrease in the C and N peaks than the Ar 150 W sample.

The decrease in C and N surface concentrations is probably due to surface coverage by Sn and Pd, while the O intensity increased due to the bonding of atmospheric oxygen to the Sn, or air oxidation of the tin forming higher order oxides. The oxygen core-level spectrum indeed shows a significant increase in the oxygen-metal bonding. The oxygen spectrum (not shown here) also showed a significant decrease in the relative fraction of O═C and an increase in the O–C bonding, indicating that Sn interacts with surface oxygen on the PI surface at the C═O sites. This is further supported by the shift in the Sn binding energy from 485.1 eV for metallic Sn to 486.8 eV for Sn^{+2} (corresponding to Sn–O bonding[24]), as shown in Fig. 9. The Sn core-level XPS spectra for three plasma-treated surfaces are shown in Fig. 9. Only the NH_3 80 W sample shows the presence of a small amount of metallic Sn (peak 2 in Fig. 9A). The

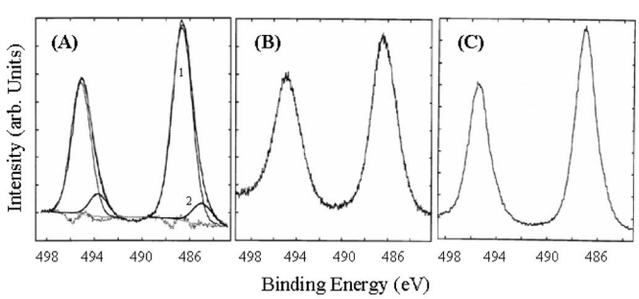

Figure 9. Core-level XPS spectra of Sn on PI surface with three different plasma treatments: (A) NH_3 80 W; (B) Ar 150 W; and (C) Ar 150 W + NH_3 30 W.

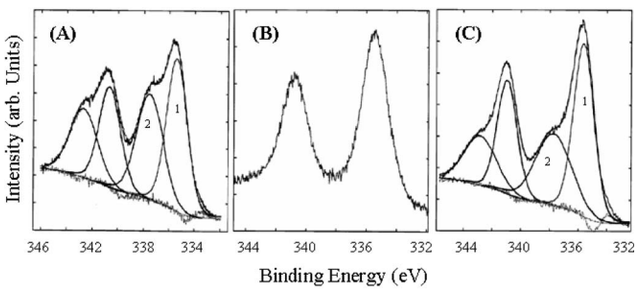

Figure 10. Core-level XPS spectra of Pd on PI surface with three different plasma treatments (A) NH_3 80 W; (B) Ar 150 W; and (C) Ar 150 W + NH_3 30 W.

Ar plasma and Ar + NH_3 plasma samples show only Sn(II). The Sn bonding behavior on the PI surface is consistent with the literature reports.[21] However, the amount of Sn adsorbed on the surface does not seem to correlate with the oxygen surface concentration. A greater amount of Sn (20–28%) is observed for the NH_3 80 W and Ar + NH_3 samples, while the NH_3 30 W and Ar plasma-treated samples show surface Sn concentrations of only about 7-8%, as shown in Table I. The oxygen surface concentration was in the 20-25% range for all samples prior to the Sn–Pd treatment.

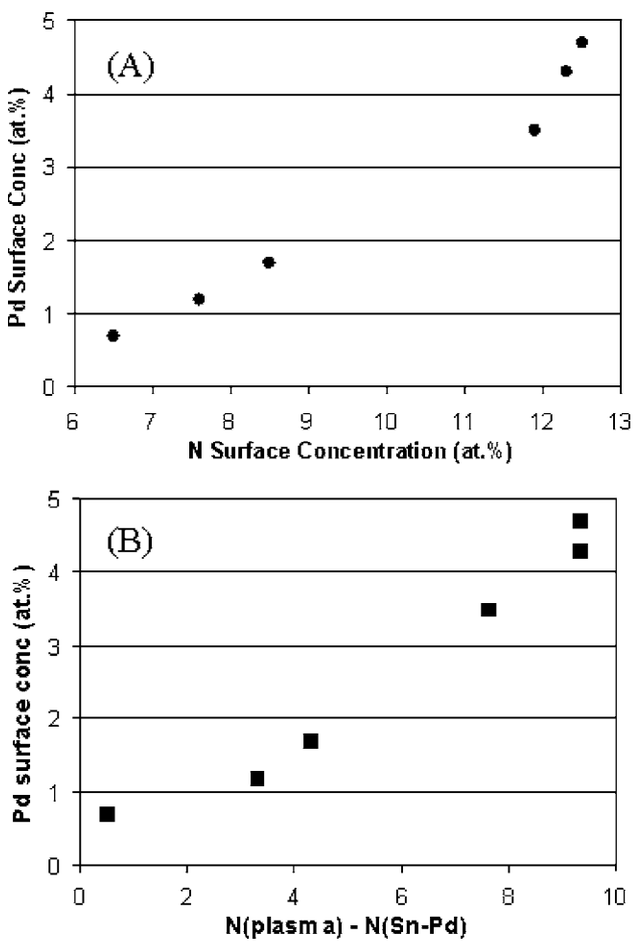

Figure 11. Correlation between (A) N surface concentration and amount of Pd adsorbed and (B) reduction in N surface concentration and amount of Pd adsorbed.

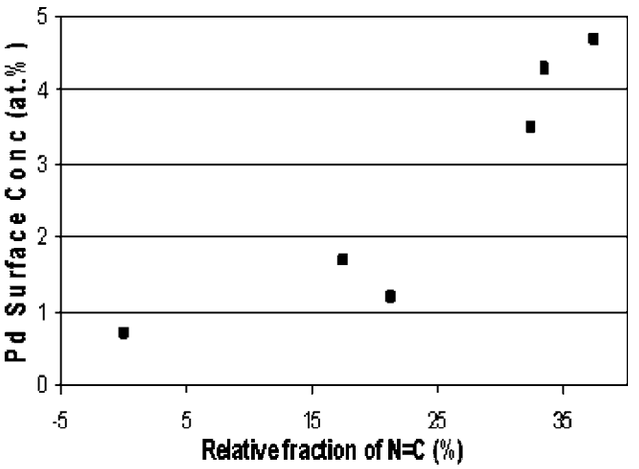

Figure 12. Correlation between relative fraction of N═C and Pd surface concentration.

The amount of Pd adsorbed on the surface, however, is much lower than that of Sn, again consistent with previous reports.[21,24] The Pd XPS core-level spectra, Fig. 10, show that Pd has two bonding states: 335.5 eV (peak 1) corresponding to Pd^0 and 337.7 eV[23] (peak 2) corresponding to Pd(II) for the NH_3 plasma treatment. Only the metallic state was observed in the Ar 150 W sample. The Pd(II) fraction was 47% for the NH_3 80 W sample and 41% for the Ar 150 + NH_3 30 W sample. The binding energy of the Pd(II) component (peak 2) seen in the NH_3-treated samples in this study was at 337.7 eV, which is slightly lower than Pd–O bonding at 338.5 eV. This leads us to believe that the Pd(II) state observed may correspond to Pd–N bonding, because nitrogen has lower electronegativity than oxygen and as a result would have a lower shift in the Pd binding energy. The unbonded electron pairs on the oxygen and nitrogen are the interaction site. Additional support for the Pd(II) state in the form of a Pd–N bond is shown in Fig. 11. The surface concentration of Pd is plotted as a function of N concentration which existed prior to the application of the Sn–Pd treatment in Fig. 11A. The concentrations of Pd and N were determined from the integrated areas under their respective photoelectron peaks and the sensitivity factors (photoelectron emission cross section), as mentioned in the Experimental section. The effects of variations in the XPS sampling depth with Sn and Pd coverage were not taken into account. The direct relationship between these two quantities in Fig. 11A supports the correlation between the surface nitrogen concentration and resulting Pd for all the plasma treatments. The surface nitrogen is an effective site for nucleation of the Pd catalyst. Furthermore, the number of available nitrogen sites is lowered by the Sn–Pd treatment ($N_{plasma} - N_{Sn-Pd}$) and plotted against the Pd content for all plasma treated samples in Fig. 11B. The direct correlation in Fig. 11B also suggests that the lowering of the nitrogen surface concentration is due to coverage of the nitrogen by palladium. Moreover, it was also observed that a direct correlation exists between the relative fraction of the N═C bonding (399.5 eV peak in the N spectrum) and the surface concentration of Pd, as plotted in Fig. 12.

Figures 11 and 12 support the concept that the Pd is bonded to N (via the unbonded electon pairs), specifically in the N═C configuration, which is produced by the NH_3 plasma treatment and also by Ar plasma treatment through nitrogen surface rearrangement. The interaction of Pd with N═C is independent of the plasma treatment that the surface has received.

The electroless copper plating occurred after the Sn–Pd activation process. The Sn–Pd activated samples were immersed in the copper plating bath for a few seconds, just long enough to deposit a few monolayers of Cu so that the bonding states of Cu at the inter-

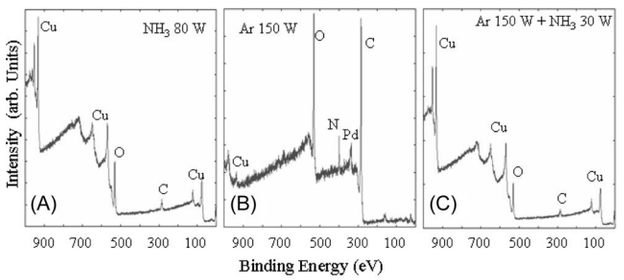

Figure 13. XPS survey scans after 5 s electroless Cu deposition for different plasma treatments: (A) NH_3 80 W; (B) Ar 150 W; and (C) Ar 150 W + NH_3 30 W.

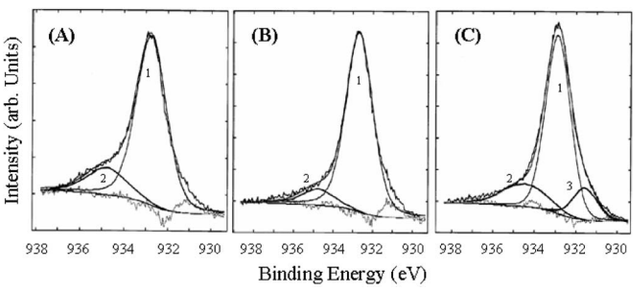

Figure 14. Core-level XPS spectra of Cu on PI surfaces with different plasma treatments: (A) NH_3 80 W; (B) Ar 150 W; and (C) Ar 150 W + NH_3 30 W.

face could be analyzed by XPS. The XPS survey scans after 5 s of electroless copper plating, for the three different plasma treatments, are shown in Fig. 13.

The Cu^0 peak at 932.8 eV is present on the samples having received the NH_3 plasma treatment, whereas it is very weak on the Ar 150 W sample. The amount of Cu deposited on the surface, calculated as a fraction of surface coverage, for different plasma treatments and deposition times is given in Table II. This shows that, for samples that received only the Ar plasma treatment, 0.3-0.4% of the surface is covered with Cu in the first 5 s. On the NH_3 80 W and Ar + NH_3 samples, 20-30% of the surface is covered with Cu in the same 5 s plating time. The NH_3 30 W sample falls between the two extremes with 4.9% Cu coverage for the 5 s plating experiment. With longer deposition times, the Cu surface coverage increases for the NH_3 30 W and Ar plasma samples.

The core-level XPS spectra for copper are shown in Fig. 14. These spectra show that copper has two bonding states in the NH_3- and Ar-plasma treated samples. The dominant peak at 932.7 eV (peak 1) corresponds to Cu^0 and the second peak at 934.8 eV (peak 2) corresponds to the Cu–O bonding.[24] This oxygen is believed to be due to air oxidation covering the Cu surface after plating. The oxygen peak (not shown) displays a strong oxygen-metal content at 530.5 eV. The Ar + NH_3 plasma sample contains a third peak at 931.6 eV (peak 3) which is due to Cu–Pd bonding.[24] This peak is prominent in all the samples that received the combined plasma treatments, while it is weak (but present) in the samples that received only the NH_3 or Ar plasma treatments. The spectra in Fig. 14 clearly show that a dominant fraction of Cu is in a metallic state regardless of the plasma treatment.

The increase in Cu surface coverage for this sample with plating time is plotted in Fig. 15. The surface coverage increases with plating time, but is nonlinear because electroless copper is an autocatalyic process. The rate of plating increases with the amount of Cu present on the surface.

Table II shows that the copper coverage of the PI (as a function of electroless deposition time) depends on the surface pretreatment.

Table II. Surface composition of PI (in atom %) after various plasma treatments and different electroless Cu deposition times.

Surface Treatment		C	O	N	Sn	Pd	Cu
Theoretical		78.1	15.6	6.2			
No Treat		80.3	15	4.1			
30 W NH_3		61.1	24.8	8.8			
	Sn–Pd	44.8	40.9	4.5	7.9	1.7	
	Cu (5 s)	61.3	28.1	4.3	—	1.3	4.9
	(10 s)	66.7	25.6	2.2	—	—	5.5
	(20 s)	53.1	34.1	3.8	—	—	9.1
	(30 s)	34.2	45.2	0.7	—	—	19.9
80 W NH_3		66.4	20.4	12.3			
	Sn–Pd	34.2	41.8	3.3	16.2	4.3	
	Cu (5 s)	32.2	45.9	1.3	—	—	20.6
50 W Ar		69.1	24.9	6.5			
	Sn–Pd	55.9	30.1	6	7.3	0.7	
	Cu (5 s)	73.2	21.4	5.1	—	0.6	0.3
	(30 s)	49.8	35.3	3.6	—	—	9.95
150 W Ar		66	22.9	7.6			
	Sn–Pd	58.4	28.6	4.3	7.6	1.2	
	Cu (5 s)	70.6	22.5	5.5	—	1	0.4
	(30 s)	28.6	45.2	1.5	—	—	24.7
50Ar + 30NH		64.8	23.2	11.9			
	Sn–Pd	33.7	39.7	4.3	17.6	3.5	
	Cu (5 s)	34.9	44.3	—	—	—	20.9
150Ar + 30NH		62.4	21.4	12.5			
	Sn–Pd	31.7	40.5	3.2	21.1	4.7	
	Cu (5 s)	26.9	45.7	—	—	—	27.4

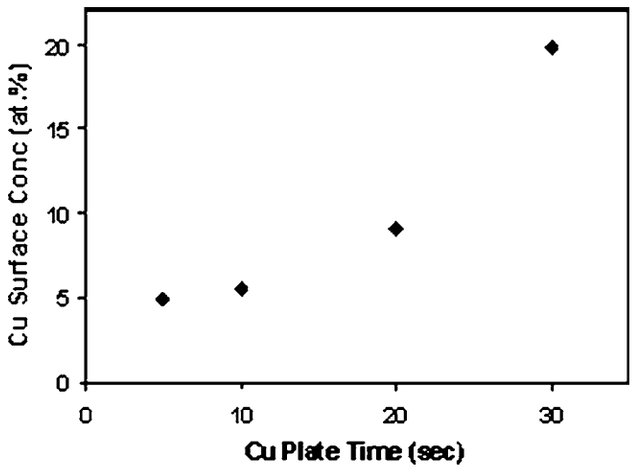

Figure 15. Progression of Cu surface coverage of the NH_3 30 W sample with electroless plating time.

Figure 16 shows the relationship between Pd surface concentration and Cu coverage. There is a linear relationship between the Pd concentration on the surface and Cu coverage for the initial stage of electroless deposition, because Pd is the catalyst for the process. We have noted before that the Pd surface concentration is linearly proportional to the N (specifically –N═C< on the surface). Thus, the Cu coverage should also be directly related to the concentration of N═C on the plasma-treated PI surface.

Peel tests were performed to measure the adhesion strength of the copper to the PI for the different plasma treatments. Untreated PI samples do not undergo electroless copper activation with Sn–Pd and were therefore not analyzed. Table III shows the results for four electrolessly plated samples. As mentioned before, ~40 μm of Cu was electroplated on 0.6 μm electroless Cu in order to be able to pull the tab. The peel-test values achieved in this study (33–65 N/m) are lower compared to those on electrolessly plated epoxy substrates (~460 N/m). However, there is a definite improvement in this peel strength from the Ar-plasma-treated to the combined plasma-treated sample (from 33 to 65 N/m). These two samples have similar roughness values but very different peel strengths, which shows that roughness alone is not sufficient for high adhesion. A combination of roughness and chemical modification is needed for maximum adhesion. The magnitude of roughness

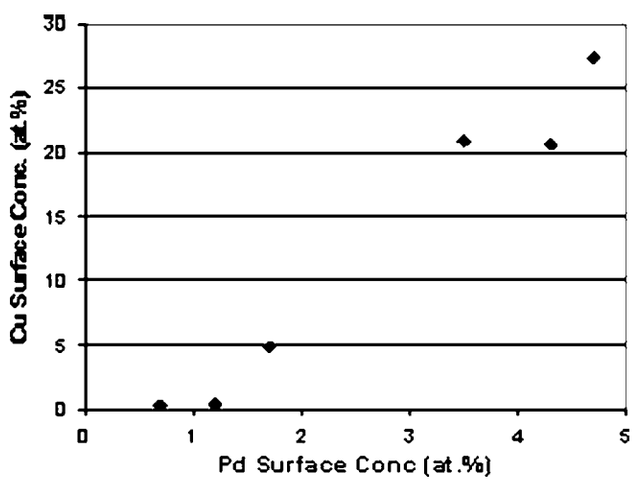

Figure 16. Correlation between Pd surface concentration and Cu surface coverage.

Table III. Results of electroless Copper peel tests on PI samples subjected to different plasma treatments.

Pretreatment	RMS roughness (A)	Peel strength (N/m)
Ar 150 W	175.5	33
NH_3 30 W	12	38
NH_3 80 W	29.3	64
Ar 150 W+NH_3 30 W	180.1	65

obtained on PI by plasma treatments in this study (of the order of 200 A) is more than one order of magnitude lower than the roughness obtained on epoxy prior to electroless Cu plating (typically 7000–8000 A). Consequently, the adhesion of electroless Cu on epoxy is about an order of magnitude higher than on PI. The present results show that, for a given magnitude of surface roughness, improvement in chemical bonding improves the adhesion by at least a factor of 2, and that adequate adhesion can be obtained without aggressive destruction of the surface to create very high roughness.

Analysis of the PI and Cu surfaces after peel tests are shown in Fig. 17 for the NH_3 30 W plasma-treated sample. This figure shows that the PI surface was metal-free, while the Cu surface showed the presence of Sn and Pd in addition to Cu, C, and O. This shows that adhesive failure occurred at the PI-catalyst interface. Thus, it appears that plasma treatments of the PI surface, although enabling adsorption of the catalysts for the subsequent electroless copper plating, did not enable the formation of strong covalent "adhesion" bonds between the PI surface and catalyst metals or copper.

Conclusions

NH_3 and Ar plasma treatments have been successfully used for achieving physical and chemical modifications of the PI surface, enabling electroless Cu plating. The NH_3 plasma produces chemical changes to the PI surface through insertion of N into the surface in the form of –N═C< moieties, while increasing the surface roughness by tens of angstroms. The Ar plasma treatment brings about mainly physical changes to the surface, increasing the roughness by hundreds of angstroms, while marginally increasing the oxygen and nitrogen surface concentrations through differential sputtering of carbon. The combined plasma treatment (Ar plasma followed by NH_3 plasma) combines the desirable features of both treatments, yielding a PI surface with high roughness as well as high oxygen and nitrogen surface concentrations.

During the surface activation via the Sn–Pd treatment, Sn bonds mainly with the surface oxygen, and Pd bonds with surface tin and nitrogen. A direct relationship was observed between the Pd surface concentration and the fraction of –N═C< bonding sites on the surface. This suggests that the nitrogen radicals inserted by the NH_3 plasma are effective in adsorbing Pd on the surface. Thus, the PI samples with NH_3 plasma treatment at higher power and those with

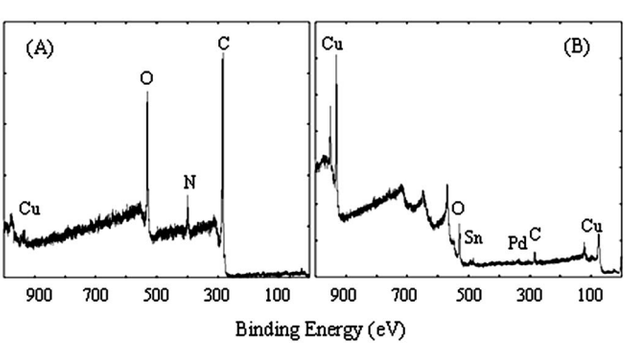

Figure 17. XPS analysis of the (A) PI and (B) Cu surfaces after peeling the Cu film.

the combined plasma treatment displayed much higher concentrations of Pd on the surface. In the subsequent electroless Cu deposition, the magnitude of surface coverage by Cu was monitored for a fixed deposition time of 5 s for different plasma-treated samples. A direct correlation between the Pd surface concentration and Cu coverage was observed.

The adhesion of Cu on the plasma-treated PI surfaces improved with the combined plasma treatments, although it was still small compared to epoxy. Analysis of the PI and copper surfaces after plating and peel testing showed that adhesive failure occurred at the PI-catalyst interface. This indicates that, although plasma treating the PI surface enables catalyst adsorption and subsequent electroless copper plating, these treatments do not yield strong covalent bonding between the PI surface and the catalyst.

Acknowledgment

Two of the authors (D.B. and H.H.) wish to acknowledge the financial support from Intel Corporation.

Georgia Institute of Technology assisted in meeting the publication costs of this article.

References

1. Z. Wang, A. Furuya, K. Yasuda, H. Ikeda, T. Baba, M. Hagiwara, S. Toki, S. Shingubara, H. Kubota, and T. Ohmi, *J. Adhes. Sci. Technol.*, **16**, 1027 (2002).
2. S. Siau, A. Vervaet, E. Schacht, and A. Van Calster, *J. Electrochem. Soc.*, **151**, C133 (2004).
3. H. Okamura, T. Takahagi, N. Nagai, and S. Shingubara, *J. Polym. Sci., Part B: Polym. Phys.*, **41**, 2071 (2003).
4. N. Inagaki, S. Tasaka, and A. Onodera, *J. Appl. Polym. Sci.*, **73**, 1645 (1999).
5. Z. J. Yu, E. T. Kang, and K. G. Neoh, *Polymer*, **43**, 4137 (2002).
6. J. Jang, I. Jang, and H. Kim, *J. Appl. Polym. Sci.*, **68**, 1343 (1998).
7. J. Seo, J. Kang, K. Cho, and C. Park, *J. Adhes. Sci. Technol.*, **16**, 1839 (2002).
8. H. D. Merchant, J. T. Wang, L. A. Giannuzzi, and Y. L. Liu, *Circuit World*, **26**, 7 (2000).
9. R. F. Saraf, J. M. Roldan, and T. Derderian, *IBM J. Res. Dev.*, **38**, 441 (1994).
10. S. Iwamorei, T. Miyashita, S. Fukuda, S. Nozaki, K. Sudoh, and N. Fukuda, *Vacuum*, **51**, 615 (1998).
11. F. D. Egitto and L. J. Matienzo, *IBM J. Res. Dev.*, **38**, 423 (1994).
12. Y. Nakamura, Y. Suzuki, and Y. Watanabe, *Thin Solid Films*, **290–291**, 367 (1996).
13. A. M. Ektessabi and S. Hakamata, *Thin Solid Films*, **377–378**, 621 (2000).
14. L. Zhang, T. Yasui, H. Tahara, and T. Yoshikawa, *J. Appl. Phys.*, **86**, 779 (1999).
15. R. Flitsch and D. Y. Shih, *J. Adhes. Sci. Technol.*, **10**, 1241 (1996).
16. C. Girardeaux, E. Druet, P. Demoncy, and M. Delamar, *J. Electron Spectrosc. Relat. Phenom.*, **74**, 57 (1995).
17. N. J. Chou, D. W. Dong, J. Kim, and A. C. Liu, *J. Electrochem. Soc.*, **131**, 2335 (1984).
18. L. Atanasoska, S. G. Anderson, H. M. Meyer III, and J. H. Weaver, *Vacuum*, **40**, 85 (1990).
19. M. C. Burrell, P. J. Codella, J. A. Fontana, J. J. Chera, and M. D. McConnell, *J. Vac. Sci. Technol. A*, **7**, 55 (1989).
20. J. Charlier, V. Detalle, F. Valin, C. Bureau, and G. Lecayon, *J. Vac. Sci. Technol. A*, **15**, 353 (1997).
21. M. Charbonnier, M. Alami, and M. Romand, *J. Electrochem. Soc.*, **143**, 472 (1996).
22. G. Beamson and D. Briggs, *High Resolution XPS of Organic Polymers*, John Wiley & Sons, New York (1992).
23. W. J. Lee, Y. S. Lee, S. K. Rha, Y. J. Lee, K. Y. Lim, Y. D. Chung, and C. N. Whang, *Appl. Surf. Sci.*, **205**, 128 (2003).
24. T. N. Vorobyova, *J. Adhes. Sci. Technol.*, **11**, 167 (1997).